J Comp Physiol A (1998) 182: 103–113

ORIGINAL PAPER

P. K. Stoddard

Detection of multiple stimulus features forces a trade-off in the pyramidal cell network of a gymnotiform electric fish's electrosensory lateral line lobe

Accepted: 14 June 1997

Abstract Modification of an existing neural structure to support a second function will produce a trade-off between the two functions if they are in some way incompatible. The trade-off between two such sensory functions is modeled here in pyramidal neurons of the gymnotiform electric fish's medullar electrosensory lateral line lobe (ELL). These neurons detect two electric stimulus features produced when a nearby object interferes with the fish's autogenous electric field: (1) amplitude modulation across a cell's entire receptive field and (2) amplitude variation within a cell's receptive field produced by an object's edge. A model of sensory integration shows that detection of amplitude modulation and enhancement of spatial contrast involve an inherent mechanistic trade-off and that the severity of the trade-off depends on the particular algorithm of sensory integration. Electrophysiology data indicate that of the two algorithms for sensory integration modeled here for the gymnotiform fish *Brachyhypopomus pinnicaudatus*, the algorithm with the better trade-off function is used. Further, the intrinsic trade-off within single cells has been surmounted by the replication of ELL into multiple electrosensory map segments, each specialized to emphasize different sensory features.

Key words Constraint · Electroreception · Evolution · Sensory system · Neural network

Abbreviations *AM* amplitude modulation · *CLS* centrolateral map segment · *CMS* centromedial map segment · *ELL* electrosensory lateral line lobe · *EOD* electric organ discharge · *LS* lateral map segment

P.K. Stoddard[1]
Section of Neurobiology and Behavior, Cornell University, Ithaca, New York, USA

Present address:
[1]Department of Biological Sciences,
Florida International University, Miami FL 33199, USA,
Tel.: +1-305 348-2127; Fax: +1-305 348-1986;
e-mail: stoddard@fiu.edu

Introduction

Sensory and motor systems serve as an animal's neural interface with a complex world. In those animals with a large repertoire of behaviors, the limited number of sensory and motor systems must perform multiple tasks. Motor circuits produce repertoires of effector behaviors by sequentially altering the circuit's function (Harris-Warrick and Marder 1991; Heiligenberg et al. 1996), but even if a motor system (i.e., a neural circuit that effects motor behavior) is given multiple simultaneous instructions, it cannot produce more than one functional behavior at a time. Does the same limitation on multitasking apply to sensory systems? In this paper, I consider the sensory trade-offs encountered by individual neurons in the detection of multiple stimulus features and the consequential limitations imposed by the resulting compromise. I postulate that such trade-offs constituted a selective force that has promoted the evolution of parallel structure and descending control networks in the central nervous system.

Pyramidal cells in the electrosensory lateral line lobe (ELL) of the medulla oblongata of gymnotiform electric fishes are interesting neurons in which to look for sensory coding of multiple object features. Pyramidal neurons in the ELL integrate afferent input from ganglion cells inervating tuberous electroreceptors in the skin, and fire in response to amplitude distortion of the local electric field (Bastian and Heiligenberg 1980; Bastian 1981; Saunders and Bastian 1984; Carr and Maler 1986). Gymnotiform pyramidal neurons code for changes in electric field strength resulting from the size, distance, conductivity, edge, and motion of nearby objects, as well as electric communication signals and jamming stimuli given by other electric fishes (review: Bastian 1990). Pyramidal networks in ELL are characterized both by a high degree of parallelism in connectivity and by extensive descending control networks, characteristics that have attracted considerable attention from neurobiologists.

Researchers have made some progress in understanding how pyramidal cells encode complex amplitude-modulated stimuli (Bastian 1981; Shumway 1989b; Shumway and Maler 1989; Gabbiani et al. 1996). However, existing models do not yet account for the array of responses obtained from such simple stimuli as amplitude steps. I show below that the response of pyramidal neurons in the ELL to amplitude-step stimuli sometimes makes no sense in light of our present interpretation of receptive field integration. So while we strive to understand how pyramidal neurons code for dynamic stimuli such as moving objects and communication signals, we still need to improve our understanding of how these cells encode the simplest of stimuli.

The approach I have taken here is to consider two features of an electric image: (1) its overall intensity and (2) its edge, and to model the sensitivity of a pyramidal neuron to these features under two different algorithms of sensory integration. The model identifies a key feature that distinguishes two possible algorithms of sensory integration. I present single unit physiology data from the pyramidal neurons of the gymnotiform electric fish *Brachyhypopomus pinnicaudatus* (Hypopomidae) that discriminate clearly between the two algorithms proposed.

Materials, methods and results

A model for the detection of an object's presence and edge

A pyramidal cell responds both to amplitude distortion across the entire receptive field and to contrast within the receptive field (Shumway and Maler 1989). Response to whole-field amplitude modulation (AM) is important for detection of objects and communication signals, whereas response to amplitude variation within the receptive field enhances the resolution of object edges in the context of electrolocation. Local decreases in electric field strength are produced by objects more resistive than the surrounding water, and conversely, local increases in field strength are produced by objects of greater conductivity. Proximate objects produce blurred electric field images on the fish's skin (Rasnow 1996) that may be sharpened by lateral inhibition in networks of the electrosensory CNS (Maler et al. 1981).

Detection of spatial contrast by pyramidal neurons in the ELL is made possible by antagonistic excitatory and inhibitory zones in the receptive fields of each cell, analogous to the center-surround organization of the retinal ganglion cells (Maler et al. 1981; Shumway and Maler 1989). Basilar pyramidal cells, named for their large basal dendrite, fire in response to increases in electric field intensity across their receptive fields and are inhibited by decreases (Bastian 1981; Saunders and Bastian 1984). Enhancement of edge perception is facilitated by excitatory receptive field centers and inhibitory receptive field surrounds (Fig. 1) (Bastian 1986a; Shumway and Maler 1989). Non-basilar pyramidal cells lack the basal dendrite, show the opposite pattern of response, and receive the opposite pattern of receptive field input.

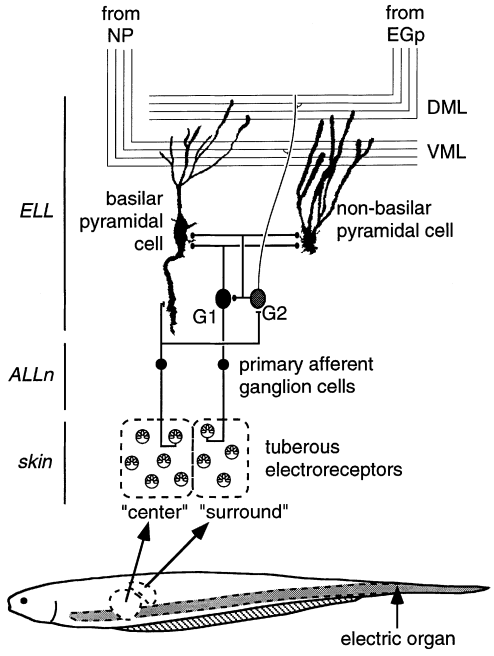

Fig. 1 Schematic of the partial circuit of pyramidal neurons in the ELL of a gymnotiform electric fish (adapted from Maler et al. 1981; Maler and Mugnaini 1994). Two pyramidal cells of *Brachyhypopomus pinnicaudatus* are reconstructed here from three serial sections containing two units filled with lucifer yellow. Pyramidal cell axons are not shown. Excitatory synapses are depicted by *bars* and inhibitory synapses by *black ovals*. Note that a pyramidal cell's receptive field "surround" does not fully surround the center as it does in the retinal ganglion cell. *ALLn* Anterior lateral line nerve, *ELL* electrosensory lateral line lobe of the medulla oblongata, *G1* type I granule cell, *G2* type II granule cell, *DML* dorsal molecular layer, *EGp* eminentia granularis posterior, *PD* nucleus praeminentialis dorsalis, *VML* ventral molecular layer

Spike rates of amplitude-coding tuberous electroreceptive afferents approximate logistic functions of the intensity of the preceding electric organ discharge (EOD; Fig. 2) as observed by Suga (1967). I modeled ascending inputs to the pyramidal cell by combining primary afferents and granule cell interneurons into a pair of logistic functions representing the input from center and surround receptive fields (Fig. 3, column 1):

$$N = \frac{K}{(1 + e^{(a-ri)})} + y \qquad (1)$$

where $N =$ number of spikes per stimulus event, $K =$ magnitude of the response, $y =$ lower asymptote of N, $r =$ dynamic range of N, $a =$ response threshold, and $i \approx$ stimulus intensity.

I modeled pyramidal cell response to brief stimulation of the entire receptive field (Fig. 3, column 2) as the difference between response of the two input functions (e.g., center minus surround). Response to AM of the entire receptive field (Fig. 3, column 3) was calculated the same way, except that the baseline stimulus intensity

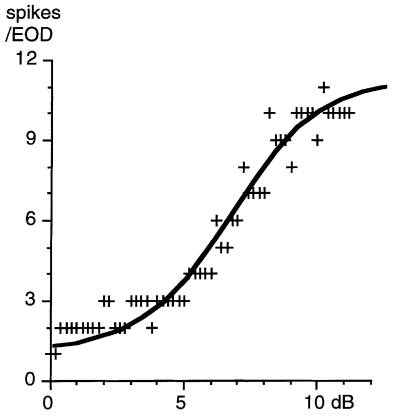

Fig. 2 Spikes per burst (+ symbols) given by a typical amplitude-coding primary afferent ganglion cell (burst-duration coder) of *Brachyhypopomus diazi* (adapted from Yager and Hopkins 1993). Electric stimuli were single-period sinusoids presented at various amplitudes. The logistic curve (*solid line*) makes a good approximation of the input from the electroreceptive periphery to the pyramidal neurons of the ELL

was chosen to be that producing the greatest slope. I modeled response to contrast within the receptive field (Fig. 3, column 4) by assigning a constant baseline stimulus intensity to the center input function and modulating the stimulus intensity of the surround function by increments up to ±1 dB. The baseline intensity was set to the steepest point in the slope of the AM response curve, about 5.5 dB.

The model shows that because center and surround inputs are antagonistic, a pyramidal neuron would be most sensitive to AM if it integrated afferent input from the center receptive field and ignored competing input from the receptive field surround (Fig. 3A). In this reduced capacity, a pyramidal cell would act as a simple spatial integrator. While response to overall AM would be optimal, detection of contrast within a receptive field is impossible with no opposing surround function. Addition of an antagonistic receptive field surround of equal but opposing magnitude (Fig. 3B) provides unidirectional sensitivity to edge contrast, but eliminates response to overall AM. For pyramidal cells to detect

Fig. 3 Models of basilar pyramidal cell response to (1) brief bursts of stimuli, (2) amplitude modulation of a steady stimulus, and (3) amplitude contrast within the receptive field. Model **A** optimizes sensitivity to stimulation of the entire receptive field by nulling the surround input function ($K_s = 0$ in Eq. 1). Only the excitatory receptive field center provides input to the cell; thus the cell's output matches its input. Model **B** includes a surround function identical to its center function. The cell becomes insensitive to simple stimulation or AM of its entire receptive field but can detect limited spatial contrast in which the center receives stronger input than the surround. Models **C** and **D** illustrate two possible strategies for compromise between sensitivity to whole-field AM and edge contrast. In model **C**, the magnitude of the receptive field surround input is smaller than that of the receptive field center ($K_c = 1, K_s = 0.75$). In model **D**, receptive field center and surround have identical magnitude but different thresholds (ac = as−3 dB). The predicted response to brief stimulus bursts (*column* 2) and AM stimuli (*column* 3) is Gaussian instead of monotonic resulting in potential ambiguity between responses to particularly high and low intensity stimuli

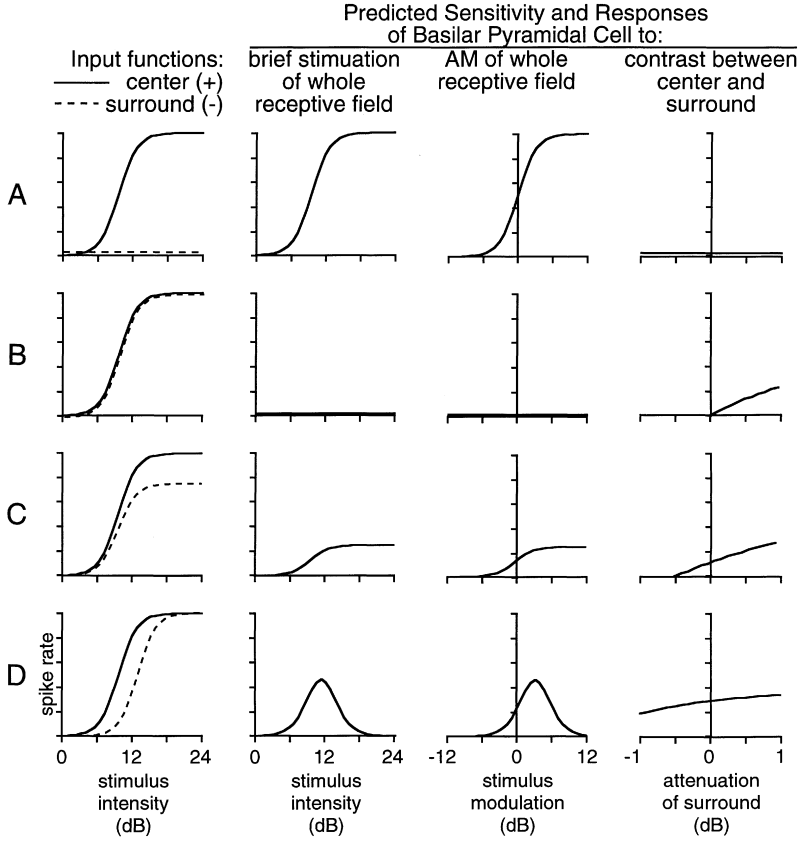

AM and enhance detection of edges concurrently, the pyramidal cell must assign more weight to input from the receptive field center than to the surround (Bastian and Heiligenberg 1980; Bastian 1986a, b; Shumway and Maler 1989). The necessary weighting function can take either of two forms: in the "attenuated surround" model (Fig. 3C), the surround input function has lower gain than the center input function. In the "shifted surround" model (Fig. 3D), the surround input function has the same total dynamic range as the center input function but has a higher stimulus threshold. These two trade-off models produce qualitatively different output functions in response to stimulation (Fig. 3, column 2) or modulation (Fig. 3, column 3) of the entire receptive field. Attenuation of the surround function magnitude results in a logistic response curve (Fig. 3C) whereas increasing the surround threshold produces a Gaussian-shaped response curve (Fig. 3D).

Simulation of sensitivity to AM and enhancement of contrast (Fig. 4) shows the forced trade-off between sensitivity to these two features of an electrosensory stimulus. In both models, where center and surround input functions are similar, edge enhancement dominates and whole-field sensitivity is absent. As input functions diverge, whole-field response increases steeply in the shifted surround model and gradually in the attenuated surround model. In the attenuated surround model, sensitivity to AM stimuli trades off unit-for-unit with edge enhancement. The shifted surround model produces a slightly better compromise, seen in the difference between the sums of the curves in Fig. 4.

The algorithm of input integration, either attenuated or shifted surrounds, should be revealed by silencing the natural EOD and examining the response of pyramidal cells either to brief bursts of synthetic EODs of different amplitudes, or to brief AMs of a synthetic EOD. A strictly monotonic response curve would support the attenuated surround model, whereas a diminished response at higher stimulus intensities would support the shifted surround model. I silenced the electric organ with curare and recorded action potentials from individual pyramidal cells while stimulating the fish as described below.

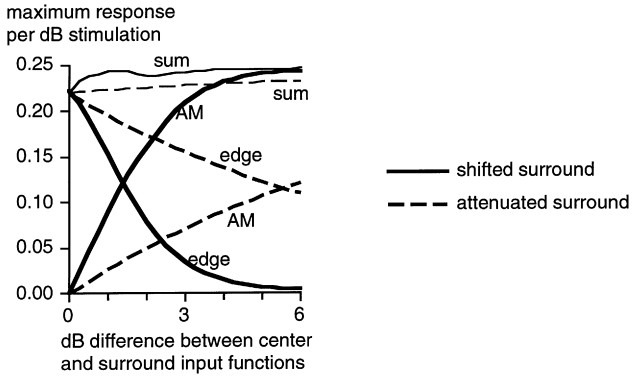

Fig. 4 Model of the response to whole-field AM and within-field contrast as the surround input function is either attenuated relative to the center input function (Fig. 3C), or shifted upwards in dynamic range (Fig. 3D). Trade-offs between the responses to AM and edge stimuli are readily apparent in both models. Comparison of the 'sum' curves produced by summing the AM and edge detection functions for each model shows that the shifted surround model affords a slightly better compromise than the attenuated surround model

Physiology methods

I made extracellular recordings of 124 pyramidal units in the lateral and centrolateral ELL map segments of 60 adult *Brachyhypopomus pinnicaudatus* (Gymnotiformes: Hypopomidae) (Hopkins 1991), a South American weakly electric fish with a pulsed EOD. [Systematics note: the genus *Brachyhypopomus* includes all species previously described under the genus *Hypopomus* except for a couple of long-nosed species from the coastal streams of the Guianas (Mago-Leccia 1994)]. Prior to recording, I digitized the fish's EOD and measured its field intensity from a location just posterior to the operculum where the field vector is primarily lateral in direction (P. Stoddard, B. Rasnow, C. Assad, unpublished observations). I tranquilized the fish with a 1-min immersion in a weak (10 mg l^{-1}) buffered MS-222 solution, then immobilized it by injecting 40–60 μg of the synthetic curare Flaxedil (gallamine triethiodide), also abolishing the natural EOD. I suspended the fish at the surface of a round tank (46 cm diam., 13 cm deep) so that just the top of the head was exposed. A recirculating system delivered aerated water (28 °C) to the fish's mouth. Water conductivity was 200 μSm^{-1}. I applied lidocaine to the exposed skin, glued a small post to a section of exposed parietal bone to stabilize the skull, and opened a hole (1 × 2 mm) in the skull to expose the ELL. I recorded from single pyramidal cells in the lateral and centrolateral somatotopic map segments of the ELL using extracellular metal-filled glass pipettes (adapted from Dowben and Rose 1953).

A window discriminator detected action potentials which, along with stimulus event times, were recorded online by a home-made computer interface with submicrosecond resolution. Resynthesized EODs were delivered through a pair of transformer-isolated electrodes, one a silver ball placed in the pharynx, the other a silver ring around the tip of the fish's tail. This electrode geometry produced a reasonable EOD replicate only over the anterior third of the fish so I restricted my recording to anterior regions of the ELL receiving afference from this region. I adjusted initial EOD amplitude to match that recorded prior to curarization.

A data record included response to 50 stimulus cycles. *Burst stimuli*: 0.5-s bursts of synthetic EODs delivered every 2.5 s at a rate 30 EODs s^{-1}, the fish's resting discharge rate. I varied the stimulus over the range in which spike rates differed significantly (*F*-test, $a = 0.01$) over three 0.5-s phases: before, during, and after stimulation. *AM stimuli*: amplitude modulation (±1, 2, 4, 6 dB) of one EOD per second in a steady series of EODs delivered at a rate of 30 EODs s^{-1}. Response to

AM, defined as all spikes recorded in the 1/30 s between the AM EOD and the next EOD of normal intensity was contrasted with the spike rates in the periods before and after. After every data record, I increased or decreased the stimulus intensity and allowed the cell to adapt for 60 s before collecting a new record. To be sure that pyramidal cells were giving a consistent, repeatable response throughout a data series, I ran at least one stimulus intensity at both the beginning and the end of a data series. If the response changed dramatically, I discounted the data and repeated the series or looked for a new cell.

Receptive fields of some units were mapped with the aid of a 1-mm dipole stimulating electrode. The field was first located by hand, then mounted in a manipulator for precise measurement of the receptive field center and surround. While receptive fields were easy to locate by this method, local stimulation during mapping often caused receptive fields to shrink and in some cases to disappear entirely, probably nulled by the descending control system.

The ELL laminae of *Brachyhypopomus* are not flat as seen in the gymnotiform genera *Eigenmannia* and *Apteronotus* (Carr and Maler 1986; Maler et al. 1991) but rather curve around laterally and caudally to form a cup (Fig. 5). Thus, a single electrode penetration on the lateral edge may intercept pyramidal cells in both the lateral and centrolateral maps of the ELL. Extracellular recording location was confirmed by electrolytic lesion and subsequent inspection of the sectioned brain. I filled a small number of cells intracellularly with lucifer yellow dye to confirm that the two physiologically distinctive pyramidal cell types, as determined by their response to an abbreviated burst stimulus regime, matched their presumptive basilar and nonbasilar morphological types (Fig. 1).

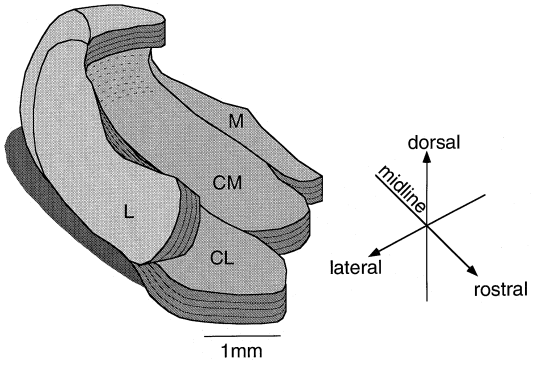

Fig. 5 The geometry of the *Brachyhypopomus* ELL is shown here, reconstructed from camera lucida tracings of fixed sections (25 μm) stained with cresyl violet. The ELL of gymnotiform fishes includes four electrosensory maps of the body surface. The medial map segment receives afference from the ampullary electroreceptors and the outer three map segments receive afference from the tuberous electroreceptors. The ELL segments in this genus do not lie flat, but form a cup wherein the outer two segments curve up and around the lateral and caudal surfaces of the medullar protuberance

Physiology results

Basilar pyramidal cells responded to burst stimulation with an increase in spike probability during the stimulus period, followed by a slight depression in spike probability for a similar period afterwards (Fig. 6). Response was often tonic over the 0.5-s periods of stimulation, consistent with findings in gymnotiform families with wave-type discharges (Bastian 1981; 1986a). Non-basilar pyramidal cells were suppressed by burst stimulation and discharged strongly immediately after cessation of the stimulus (Fig. 6).

Responses of basilar pyramidal cells to stimulus bursts were not monotonic functions of stimulus intensity (Fig. 7a), but rather approximated the Gaussian shape expected if the center and surround input functions are offset in their dynamic ranges in accordance with the shifted surround model of Fig. 3D. Responses were sharply attenuated at higher stimulus intensities, and were actually suppressed below the spontaneous rate at the highest stimulus intensities. The post-stimulus rebound patterns of non-basilar pyramidal cells were likewise non-monotonic functions of stimulus intensity (Fig. 7a) , similar to the stimulus response curves of the basilar pyramidal cells.

Response to AM stimulation was generally like that shown for pyramidal cells of the gymnotiform species with wave-type discharges (Fig. 8). Basilar pyramidal cells usually responded to AM of a single EOD with an increase in spike probability for positive AM and with a decrease in spike probability for negative AM. Non-

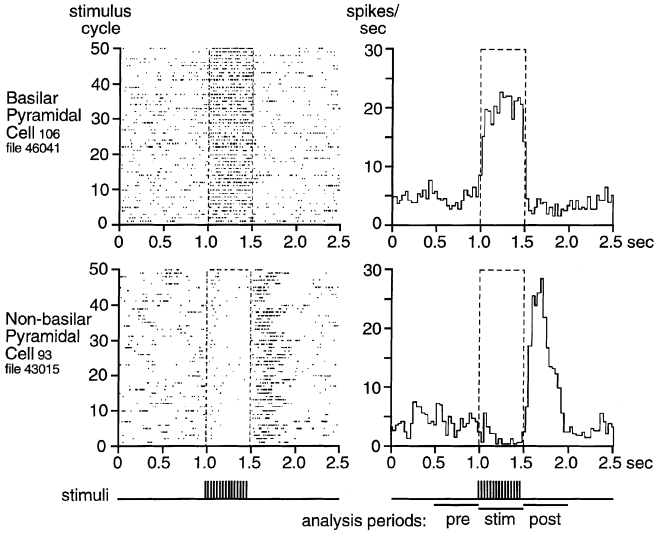

Fig. 6 Raster plots and peri-stimulus time histograms of basilar and non-basilar pyramidal cells stimulated with bursts of synthetic EODs as shown. Basilar pyramidal cells show an excitatory response that is tonic over the 0.5-s period of stimulation, followed by a similar period of weak suppression. Non-basilar pyramidal cells are suppressed by simulation and show a strong phasic rebound lasting about the same duration as the period of stimulation. Shorter periods of stimulation produced shorter-lasting post-stimulus rebounds. Cells 106 and 93 were in the centrolateral map segment

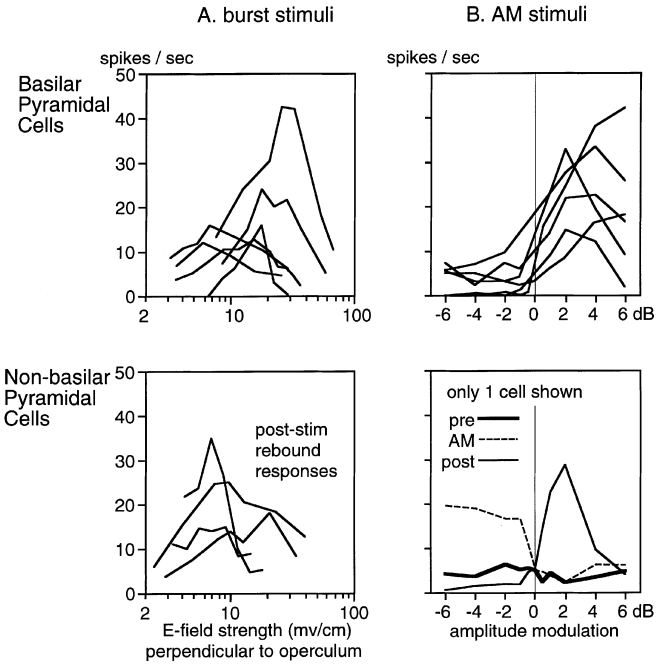

Fig. 7 Discharge functions of individual pyramidal cells stimulated with (**A**) bursts of synthetic EODs or with (**B**) amplitude modulation (*AM*) of one EOD per second presented in a steady series of synthetic EODs. The 0 dB baseline in the AM presentations was set to match the natural EOD prior to curarization. Non-monotonic response to bursts and AM stimuli support the shifted surround model in which surround input functions to the pyramidal cells are shifted upward in dynamic range (e.g., Fig. 3D). Response shown for basilar pyramidal cells is the discharge rate during the stimulus and AM periods. Response of non-basilar pyramidal cells is more complicated. Post-stimulus rebound characterizes the response to burst stimulation as shown here by the mean spike rate during the 0.5-s post-stimulus period. The timing of discharge in response to AM stimuli depends on the sign of the modulation. Reduction in stimulus amplitude produced a strong monotonic response during the stimulus period (*dashed line*), whereas an increase in stimulus amplitude produces a post-AM rebound (*thin solid line*) that varies non-monotonically with AM intensity. Response to both types of stimulation was non-monotonic (apparent exceptions are explained in the text)

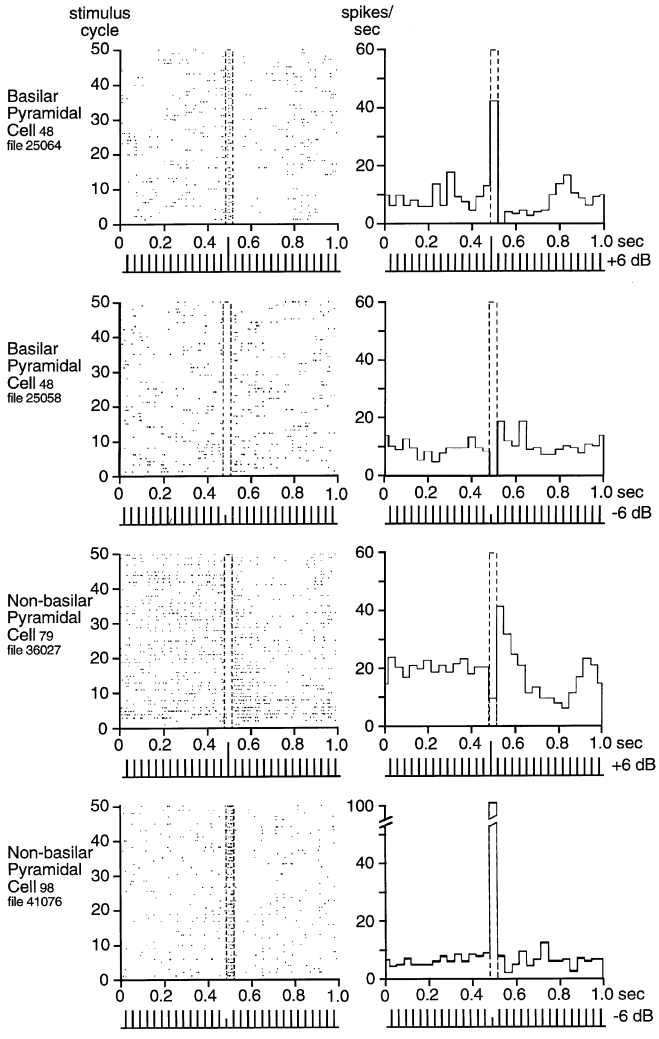

Fig. 8 Raster plots and peri-stimulus time histograms of basilar and non-basilar pyramidal cells stimulated with an amplitude step modulation (AM) of one EOD per second. Both cell types showed strong response to amplitude step modulation of a single EOD. Basilar pyramidal cells responded to positive AM steps with a sharp increase in spike rate, usually followed by suppression and gradual recovery. Negative AM steps produced brief suppression and a small rebound. Non-basilar pyramidal cells were suppressed by positive AM steps and gave significant post-stimulus rebound that outlasted the stimulus several times over. Negative AM steps produced strong excitation but no particular rebound (see also Fig. 7b). Responses varied qualitatively from cell to cell and over small differences in stimulus intensity. The basilar pyramidal data shown here (cell 48) responded sharply to both polarities, but I could not find a non-basilar pyramidal that did so. Individual pyramidal cells tended to give big responses to large steps of positive or negative but generally not both, for reasons that will become apparent in Fig. 9. Cells 48 and 79 were in the lateral map segment and cell 98 was in the centrolateral map segment

basilar pyramidal cells were excited by negative AM stimulation and showed strong post-stimulus rebound following positive AM stimulation.

In most cases, response of basilar pyramidal cells to AM stimulation was attenuated at higher AM stimulus intensities (Fig. 7b) as it was during burst stimulation. In those few basilar pyramidal cells where response was monotonic, the high response thresholds of those cells suggest that the strongest AM stimulus intensity delivered (baseline +6 dB) may not have been sufficient to reveal the drop-off in the upper ranges of their response curves. Post-stimulus rebound patterns of non-basilar pyramidal cells expressed the same non-monotonic response to stimulus intensity as the basilar pyramidal cells.

AM of longer periods (15–30 EODs – not shown here) produced a similar pattern, but also produced more adaptation and suppression of the basal discharge rate. Longer periods of stimulation needed to characterize short-term adaptation were abandoned in this experiment because they resulted in significant suppression of overall response, presumably from descending inhibition.

A key assumption of the center-minus-surround model is that a pyramidal cell's response to AM of a baseline stimulus should be determined by the shape of

the difference function as revealed through the burst-response curve. Figure 9A,B models the Gaussian center-surround difference curve to the predicted response to AM stimulation at two different baseline stimulus intensities. Model AM response curves are nothing more than segments of the center-surround difference curve re-centered vertically around some baseline spike rate. Thus, the predicted shape of the AM response function depends on where the baseline stimulus intensity falls on the center-surround difference curve. I confirmed this relationship physiologically by running a complete burst stimulus set plus two AM stimulus sets at two baseline intensities on a basilar pyramidal cell. Figure 9C,D shows how the Gaussian-shaped burst stimulus response curve of a basilar pyramidal cell relates to the shape of the obtained AM stimulation curves. For the first AM regime (Fig. 9D, left plot) I chose as my baseline intensity a stimulus amplitude midway up the rising slope of the burst stimulation-response curve. The response magnitudes surrounding that particular amplitude of stimulation was similar for both burst and AM stimulation. The basilar pyramidal cell was excited by increases in stimulus intensity and inhibited by decreases, a classic excitatory response except for the slight decline in response from +4 to +6 dB. The second AM data set (Fig. 9D, right plot) was run with a baseline intensity +5 dB higher than before, an intensity corresponding to the peak of the burst stimulation response curve. At the higher baseline intensity, the cell's response was downward rectified. Increases and decreases in stimulus intensity both attenuated the spike rate. Had I increased the baseline stimulus intensity further, shifting it farther to the right on the burst stimulation-response curve, stimulus decreases would have caused excitation instead of inhibition and the entire cell's response would be inverted. Thus, by increasing the baseline stimulus intensity, either pyramidal cell type can be made to produce a response more typical of the other: basilar pyramidal cells can be inhibited by stimulus increases

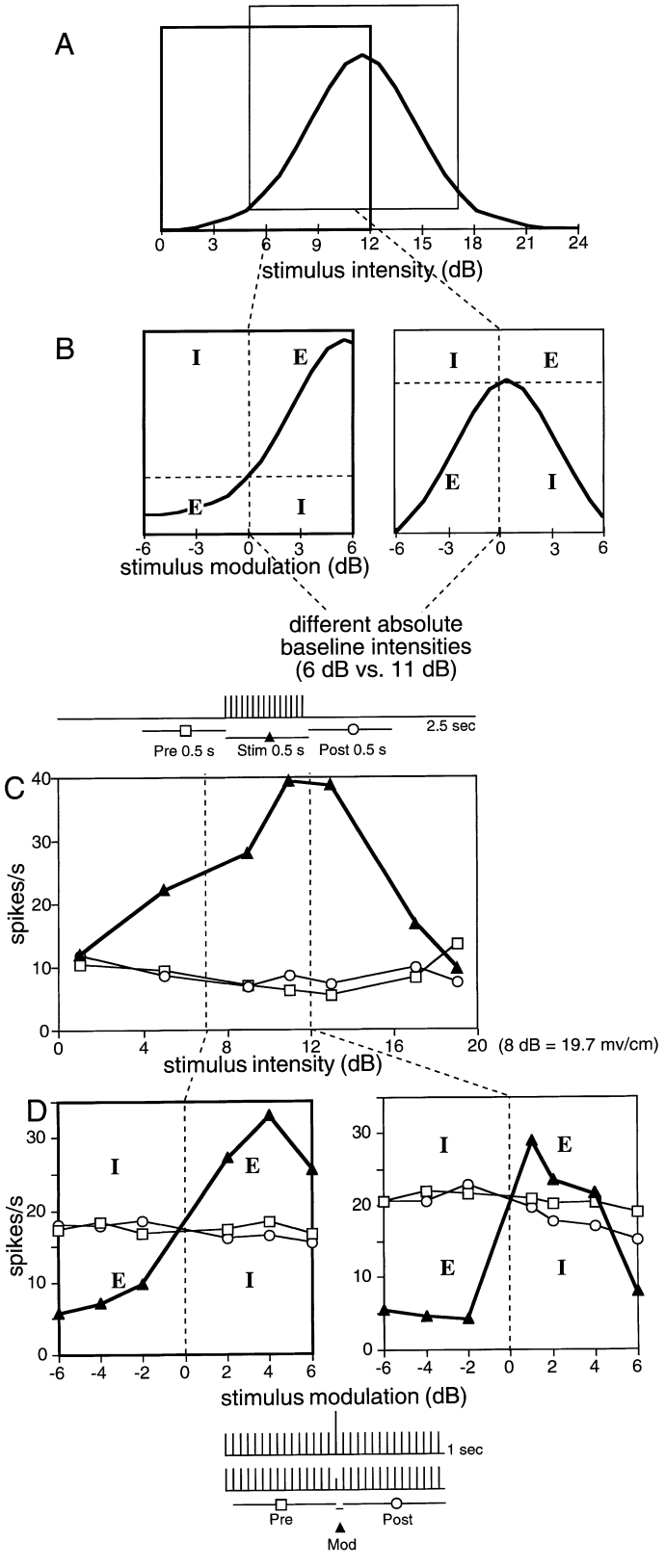

Fig. 9A Theoretical response to burst stimuli generated by the shifted-surround model can be used to predict the response of a pyramidal cell to AM stimuli. The square boxes in plot **A** delineates two 12-dB segments of the shifted-surround model's center-surround difference curve. Transposed into the format of an AM stimulus-response curve (e.g., Fig. 7b), the plot segments can be used to predict response to AM stimulation with different baseline intensities. A basilar pyramidal cell is modeled in plots **A** and **B**, and spike rates of an actual basilar pyramidal cell (106) are shown in plots **C** and **D**. The dynamic range of the model cell was scaled to match the observed dynamic range of the cell shown. Responses in the *upper right* and *lower left quadrants* of the AM subplots, designated *E*, are characteristic of excitatory cells and are typically associated with basilar pyramidal cells in the ELL. Responses in the *upper left* and *lower right quadrants*, designated *I*, are characteristic of inhibitory cells such as non-basilar pyramidal cells of the ELL. The *left side* of plot **B** shows the response of the basilar pyramidal cell to amplitude modulation of a 6-dB baseline stimulus. As expected, the cell showed a characteristic excitatory response to AM stimulation, although response to +6 dB AM was less than response to +4 dB. Increasing the baseline stimulus intensity by 5 dB to a level corresponding to the peak of the center-surround difference curve (**B** and **D**, *right plots*) inverse rectifies the cell's response. No greater response than baseline is possible and any deviation in stimulus intensity, negative or positive, produces a diminished response

and non-basilar pyramidal cells can be excited by stimulus increases.

I held one basilar pyramidal cell in the lateral segment of ELL for 2 h on the same −6 dB AM stimulus regime and collected 21 data records over a period of 110 min (Fig. 10). The cell showed a characteristic excitatory response: suppression during the AM period (1/30 s) and a strong rebound in the 1/30-s period following the AM. Of particular interest, however, the response characteristics of the cell changed spontaneously several times over the 2 h for no discernible reason (the fish had been on the rig for only 2 h and remained healthy the rest of the day). The response to baseline stimulation drifted slightly up and down, and as it did, the inhibition and post-inhibitory rebound shifted up and down in tandem. When the baseline response increased, stimulus inhibition diminished and post-inhibitory rebound dominated, a general increase in excitation. When the baseline response decreased, stimulus inhibition and post-inhibitory rebound each deviated from the baseline by similar amounts. The difference in spike rates between stimulus suppression and post-stimulus rebound remained fairly constant (mean difference = 11.6, SD = 5.0, n = 22) and both varied positively with the baseline response (r = 0.59 and 0.63, respectively, 21 *df*). Thus, when baseline response rose, the cell gave no immediate response to a dip in EOD intensity but gave an excitatory rebound equivalent to a normal response to a stimulus increase. So, during periods of increased spontaneous excitability the response to negative AM stimulation resembles the response to positive AM stimulation during periods of normal excitability; the only non-ambiguous feature of the response is the timing relative to the AM stimulus, not its direction or magnitude.

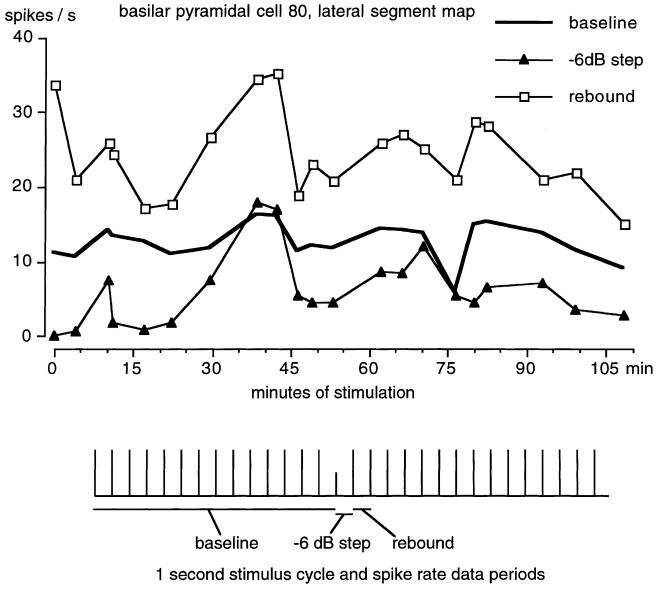

Fig. 10 Two-hour record of basilar pyramidal cell 80, stimulated continually at 30 EODs s^{-1} with a 1-s cycle of 29 EODs at 11.6 mV cm^{-1} and one EOD attenuated 6 dB. Spike rates were calculated over the following periods: *baseline* over the 14 EODs (≈467 ms) before the low intensity stimulus, *−6 dB step* over the 1-EOD period (32 ms) following the end of the low-intensity stimulus, and *rebound* over the 1-EOD period (32 ms) following the end of the next stimulus at normal intensity. Initially the cell was completely suppressed by the low-intensity stimulus, rebounding sharply upon resumption of normal stimulation. As time progressed, the baseline response drifted spontaneously up and down, accompanied by marked shifts in the excitability of the cell in response to amplitude modulation of one EOD per cycle. From 37 to 41 min, the cell showed no stimulus suppression whatsoever and rebounded sharply after the next EOD at normal intensity. This response differed from response to a +6-dB step (not shown) only in the 1-EOD period delay of the spike burst. The cell resumed its previous and more typical response pattern at 45 min but became briefly inhibited at 75 min. I show no data collected after 110 min when the cell's action potentials began to weaken

Discussion

Enhancement of edge perception requires the addition of an inhibitory receptive field surround which trades off against sensitivity to larger scale disturbances. An upward shift of the surround's dynamic range produces a more favorable trade-off in AM detection and edge enhancement than can be achieved by reducing gain of the surround, making this algorithm more favorable overall for active electrolocation. However, while an upward-shifted surround function accounts nicely for the physiology data, no such offset has been measured directly and the functional basis for an offset of the surround function is open to speculation. I suggest two hypotheses for the generation of a receptive field offset and describe evidence consistent with each. The first possibility is that offset thresholds occur at the periphery, either at the receptor or the primary afferent, and that patches of units with lower and higher thresholds project to receptive field centers and surrounds, respectively. Amplitude-coding receptor units do vary considerably in their thresholds within a fish; receptor tuning to spectral, phase, and amplitude variation in the local EOD appears to account for some but not all of the differences in receptor thresholds (Bastian 1976; Shumway and Zelick 1988; McKibben et al. 1993; Yager and Hopkins 1993). Whether units with different sensory properties are segregated by receptive field (i.e., center or surround) has not been explored. Receptive field sizes differ between pyramidal units in the different tuberous map segments of ELL (Shumway 1989a) and ganglion cells from each tuberous amplitude coder project to each map segment (Heiligenberg and Dye 1982). This pattern of parallel projection probably precludes a tight correlation between threshold and receptive field. A second hypothesis is that the dynamic range offset is generated dynamically in the network of the ELL. An effective offset of the surround's dynamic range could be achieved if type I granule cells give a non-linear response to afferent stimulation, responding more strongly to increasing stimulus intensities. Type I granule cells are normally inhibited by tonic input from polymorphic

cells of the ELL, which in turn are inhibited by increases in EOD intensity (Bastian et al. 1993). An increase in EOD intensity should disinhibit type I granule cells, perhaps amplifying the input from the receptive field surround to a point where it matches and cancels input from the receptive field center.

In other vertebrate neural networks, independent cell types are specialized for sensitivity and contrast perception. In the mammalian retina, for instance, parasol and midget ganglion cell types show different receptive field sizes and interconnectivities, apparent specializations for luminance contrast sensitivity and spatial resolution (Rodieck et al. 1985; Dacey and Brace 1992). Bastian and Courtright (1991) described a small population of deep pyramidal cells in the gymnotiform ELL that show one attribute expected of a cell type specialized for detection of whole-field AM: the location of their somata deep within ELL suggests they lack the local inhibition seen in the higher basilar and non-basilar pyramidal cell classes. However, the deep pyramidal cells give tonic response to stimulation and their apical dendrites are short and sparsely branched suggesting immunity to descending control. The tonic response shown by these cells would not be expected of a cell specialized to detect low-amplitude modulations of the receptive field, although a tonic deep pyramidal cell might relay faithfully whole-field amplitude information to an AM detector cell in the torus semicircularis. Because of the lack of surround inhibition, deep pyramidal cells should respond monotonically to increased stimulation and should not show the inverted response of the basilar and non-basilar pyramidal cells to strong stimuli. During courtship and territorial encounters, *Brachyhypopomus pinnicaudatus* frequently contact the tails of mates and rivals with their snouts (P. Stoddard, M. Kilburn, K. Patterson, unpublished observations). Because the electric field at the tails of these fish is 10–30 times stronger than at the head (unpublished observations), tuberous electroreceptors on the trailing fish's head will be driven close to saturation during these social interactions, and the associated pyramidal cells will be driven into the range of inverted response. Deep pyramidal cells are ideally suited to serve as absolute amplitude detectors capable of resolving ambiguous response in the basilar and non-basilar pyramidal cell classes.

Lacking cell classes in ELL specialized for detection of whole field AM or within-field contrast, gymnotiform fish appear to have circumvented the tradeoff at a higher level of neural integration. The gymnotiform ELL has three pairs of segments comprising parallel somatotopic map segments of the tuberous electroreceptive periphery: lateral (LS), centrolateral (CLS), and centromedial (CMS), a fourth pair of medial map segments receives input from the ampullary electroreceptors (Heiligenberg and Dye 1982). Receptive field properties of pyramidal cells vary systematically between these maps (Shumway 1989a, b). Large receptive fields of the small LS map segments optimize sensitivity to weak AM stimuli, whereas small receptive fields of the large CMS map segments facilitate spatial analysis by higher brain centers that compare output of multiple pyramidal cells. Furthermore, pyramidal cells of the LS map segment have the weakest surround inhibition and those of the CMS map segment have the strongest, suggesting that pyramidal cells of the LS map segment are specialized for overall sensitivity and those of the CMS map segment for contrast detection.

Neither physiological nor anatomical studies have looked explicitly for a dynamic link between sensitivity to whole-field stimulation and spatial contrast. Whether the trade-off between spatial contrast and whole-field sensitivity is dynamic or fixed within a single pyramidal cell thus remains open to speculation.

The descending control regions, nucleus praeminentialis dorsalis and eminentia granularis posterior, provide mechanisms by which higher brain centers might tune individual pyramidal cells dynamically to enhance overall sensitivity or detection of local contrast (Shumway and Maler 1989; Maler and Mugnaini 1994). Local application of bicuculine, a GABA-a receptor antagonist, increases contrast detection by pyramidal cells (Shumway and Maler 1989) supporting anatomical studies that suggest the center and surround input to the pyramidal cells of the ELL are under independent control (Maler et al. 1981; Maler and Mugnaini 1994). Type I granule cells control the properties of the receptive field surrounds and GABAergic type II granule cells are believed to control the properties of the receptive field centers (Shumway and Maler 1989; Maler and Mugnaini 1994). Direct descending control of type II granule cells or possibly indirect control of the less common type I granule cells via polymorphic cells could, in theory, match the strengths of center and surround inputs thereby enhancing contrast sensitivity. The descending control networks might also allow some degree of facultative optimization of individual neurons depending on particular features of interest (Crick 1984; Bratton and Bastian 1990; Maler and Mugnaini 1994).

Although the inherent intracellular trade-off between detection of AM stimuli and enhancement of edge contrast appears to have been resolved by replication of somatotopic maps, this solution was not cheap. The brain of the evolutionarily convergent mormyrid electric fish, much of which is devoted to electrosensory processing, accounts for 60% of the animal's O_2 consumption (Nilsson 1996). The rhombencephalon of the gymnotiform electric fish is greatly hypertrophied by the multiple somatotopic maps of the ELL and their associated descending control structures. Thus, the evolution of triplicate ELL maps of the tuberous electroreceptive periphery undoubtedly exacts a significant physiological cost in the metabolic support of extra brain tissue.

Pyramidal cells have been characterized as having a stereotyped response to amplitude-modulated stimuli, but under particular conditions the response patterns of basilar and non-basilar pyramidal cell types can become inverted, resembling the complementary pyramidal cell

types in their basic response patterns. Inversion of response at high baseline stimulus intensities is predicted to follow from the negative slope of the Gaussian-shaped input difference curve illustrated in the shifted-surround model. Inverted response cannot be simulated under the attenuated-surround model because the slope of the input difference curve is monotonic positive. Under the experimental AM regime, when the stimulus baseline intensity was high, perhaps supernormal, pyramidal cells showed a paradoxical response; basilar pyramidal cells were inhibited by step increases and non-basilar pyramidal cells were excited.

A second source of ambiguity in the pyramidal cell's response arises when cells become hyper-excitable, probably through descending gain control from eminentia granularis posterior (Bastian 1986a, b). An excitable basilar pyramidal cell, such as cell 80 shown in Fig. 10 at 30–40 min, would give strong responses excitatory responses to the rising edges associated with onset of positive AM and cessation of negative AM. The responses to positive and negative AMs under these circumstances would be distinguishable by the time-course of the response; response to an increase in stimulus intensity is immediate, whereas rebound response to a decrease is delayed. Pyramidal cells in the ELL follow the time-course of the stimulus (Gabbiani et al. 1996) and a basilar and non-basilar pyramidal cell pair should show temporally opposing response to any stimulus, assuming they receive similar descending control. Thus, any ambiguity in the response of a single pyramidal cell must be resolved by simultaneous comparison of basilar and non-basilar pyramidal cell output by higher neurons in the torus semicircularis.

The shifted-surround model, supported by the physiology data, produces a Gaussian-shaped response function that allows a pyramidal neuron to deliver reliable information only in the lower, positive-sloped half of its dynamic range. Electric field disturbance by nearby objects is small, generally less than a decibel (Rasnow 1996), so loss of dynamic range should impose no cost on active electrolocation. No data exist on the match between the natural baseline response of tuberous receptors and local EOD intensity in those gymnotiform fish with myogenic electric organs, all but the Apteronotidae. The Gaussian-shaped pyramidal cell response would lead me to predict that the autogenous electric field intensity lies at about one quarter of the dynamic range of the amplitude-coding tuberous electroreceptors, i.e., about 2–3 dB above threshold.

Acknowledgements I thank C. Hopkins for conceptual, technical, and financial support, S. Amagai and G. Harned for technical assistance, the late W. Heiligenberg for instruction in intracellular physiology, G. Kennedy for instruction in histology, C. Bell and J. Bastian for helpful technical suggestions, and C. Carr for moral support. C. Assad, L. Maler, M. Markham, B. Rasnow, and anonymous reviewers provided helpful comments on the manuscript. Financial support was provided by grants NIMH/NSRA-MH10149 and NIH/NIGMS-GM08205-11 to P.K.S., NIMH/NIGMS MH37972 to C. Hopkins, and NIMH/NRSA NS07303-04 to the Section of Neurobiology and Behavior at Cornell University. Experimental protocols complied with federal and local laws including the "Principles of animal care" publication No. 86-23, revised 1985 of the National Institutes for Health.

References

Bastian J (1976) Frequency response characteristics of electroreceptors in weakly electric fish (Gymnotoidei) with a pulse discharge. J Comp Physiol 112: 165–180

Bastian J (1981) Electrolocation II: the effects of moving objects and other electrical stimuli on the activities of two categories of posterior lateral line lobe cells in *Apteronotus albifrons*. J Comp Physiol 144: 481–494

Bastian J (1986a) Gain control in the electrosensory system mediated by descending inputs to the electrosensory lateral line lobe. J Neurosci 6: 553–562

Bastian J (1986b) Gain control in the electrosensory system: a role for the descending projections of the electrosensory lateral line lobe. J Comp Physiol 158: 505–515

Bastian J (1990) Electroreception. In: Stebbins WC, Berkley MA (eds) Comparative perception. II. Complex signals. Wiley, New York, pp 35–88

Bastian J, Courtright J (1991) Morphological correlates of pyramidal cell adaptation rate in the electrosensory lateral line lobe of weakly electric fish. J Comp Physiol A 168: 393–407

Bastian J, Heiligenberg W (1980) Neural correlates of the jamming avoidance response of *Eigenmannia*. J Comp Physiol 136: 135–152

Bastian J, Courtright J, Crawford J (1993) Commissural neurons of the electrosensory lateral line lobe of *Apteronotus leptorhynchus*: morphological and physiological characteristics. J Comp Physiol A 173: 257–274

Bratton B, Bastian J (1990) Descending control of electroreception. II. Properties of nucleus praeeminentialis neurons projecting directly to the electrosensory lateral line lobe. J Neurosci 10: 1241–1253

Carr CE, Maler L (1986). Electroreception in gymnotiform fish: central anatomy and physiology. In: Bullock TH, Heiligenberg W (eds) Electroreception. Wiley, New York, pp 319–373

Crick F (1984) Function of the thalamic reticular complex: the searchlight hypothesis. Proc Natl Acad Sci USA 81: 4586–4590

Dacey DM, Brace SA (1992) Coupled network for parasol but not midget ganglion cells in the primate retina. Vis Neurosci 9: 279–290

Dowben RM, Rose JE (1953) A metal-filled microelectrode. Science 118: 22–24

Gabbiani F, Metzner W, Wessel R, Koch C (1996) From stimulus encoding to feature extraction in weakly electric fish. Nature 384: 564–567

Harris-Warrick RM, Marder E (1991) Modulation of neural networks for behavior. Annu Rev Neurosci 14: 39–58

Heiligenberg W, Dye JC (1982) Labeling of electroreceptive afferents in a Gymnotoid fish by intracellular injection of HRP: the mystery of multiple maps. J Comp Physiol A 148: 287–296

Heiligenberg W, Metzner W, Wong CJH, Keller CH (1996) Motor control of the jamming avoidance responses of *Apteronotus leptorhynchus*: evolutionary changes of a behavior and its neuronal substrates. J Comp Physiol A 179: 653–674

Hopkins CD (1991) *Hypopomus pinnicaudatus* (Hypopomidae) a new species of gymnotiform fish from South America. Copeia 1991: 151–161

Mago-Leccia F (1994) Electric fishes of the continental waters of America. Biblioteca de la Academia de Ciencias Fisicales Matematicas y Naturales, vol XXIX. Caracas, Venezuela

Maler L, Mugnaini E (1994) Correlating gamma-aminobuteryc acidergic circuits and sensory function in the electrosensory lateral line lobe of a gymnotiform fish. J Comp Neurol 345: 224–252

Maler L, Sas EKB, Rogers J (1981) The cytology of the posterior lateral line lobe of high-frequency weakly electric fish (Gymnotidae): dendritic differentiation and synaptic specificity in a simple cortex. J Comp Neurol 195: 87–139

Maler L, Sas E, Johnston S, Ellis W (1991) An atlas of the brain of the electric fish *Apteronotus leptorhynchus*. J Chem Neuroanat 4: 1–38

McKibben JR, Hopkins CD, Yager DD (1993) Directional sensitivity of tuberous electroreceptors: polarity preferences and frequency tuning. J Comp Physiol A 173: 415–424

Nilsson GE (1996) Brain and body oxygen requirements of *Gnathonemus petersii*, a fish with an exceptionally large brain. J Exp Biol 199: 603–607

Rasnow B (1996) The effects of simple objects on the electric field of *Apteronotus*. J Comp Physiol A 178: 397–411

Rodieck RW, Binmoeller KF, Dineen J (1985) Parasol and midget ganglion cells of the human retina. J Comp Neurol 233: 115–132

Saunders J, Bastian J (1984) The physiology and morphology of two types of electrosensory neurons in the weakly electric fish *Apteronotus leptorhynchus*. J Comp Physiol A 154: 199–209

Shumway CA (1989a) Multiple electrosensory maps in the medulla of weakly electric gymnotiform fish. I. Anatomical differences. J Neurosci 9: 4400–4415

Shumway CA (1989b) Multiple electrosensory maps in the medulla of weakly electric gymnotiform fish. I. Physiological differences. J Neurosci 9: 4388–4399

Shumway CA, Maler L (1989) GABAergic inhibition shapes temporal and spatial response properties of pyramidal cells in the electrosensory lateral line lobe of gymnotiform fish. J Comp Physiol A 164: 391–407

Shumway CA, Zelick RD (1988). Sex recognition and neuronal coding of electric organ discharge waveform in the pulse-type weakly electric fish, *Hypopomus occidentalis*. J Comp Physiol A 163: 465–478

Suga N (1967) Coding in tuberous and ampullary organs of a gymnotid electric fish. J Comp Neurol 113: 437–452

Yager DD, Hopkins CD (1993) Directional characteristics of tuberous electroreceptors in the weakly electric fish, *Hypopomus* (Gymnotiformes). J Comp Physiol A 143: 401–414